The X-ray Perimeter Array Detector (XPAD): a New Resource for Atomic Resolution and High Sensitivity Microanalysis in the Analytical Electron Microscope

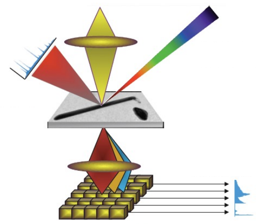

0.5 Å in TEM/STEM $\Rightarrow$ 5 Å in 5 D [X, Y, Z, S_i, τ]

Nestor J. Zaluzec
Photon Science Directorate
zaluzec@aaem.amc.anl.gov
zaluzec@microscopy.com

1

Acknowledgements

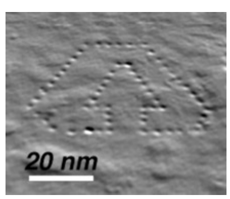

ANL LDRD Projects
ANL/ThermoFisher(FEI) CRADA #1300701

ThermoFisher SCIENTIFIC

Permission Given to Photograph/Capture Slides or Request a PDF Copy by Email

2

This Morning's Traditional Weather Report

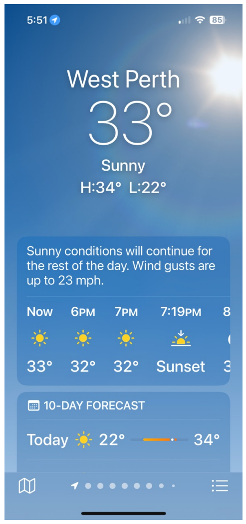

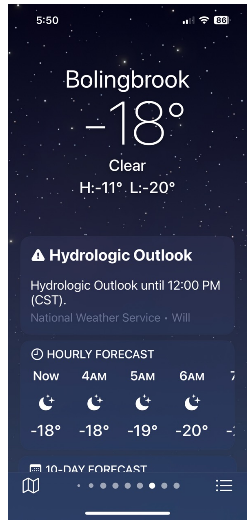

3

Last's Years Weather Report

The Year there was no meeting
Feb 2, 2022

4

Jan 25 2023
1 day prior to leaving for Oz

5

Jan 27 2023

But you managed once again to depart just in time to get out of shoveling the driveway

6

Microanalytical Challenges

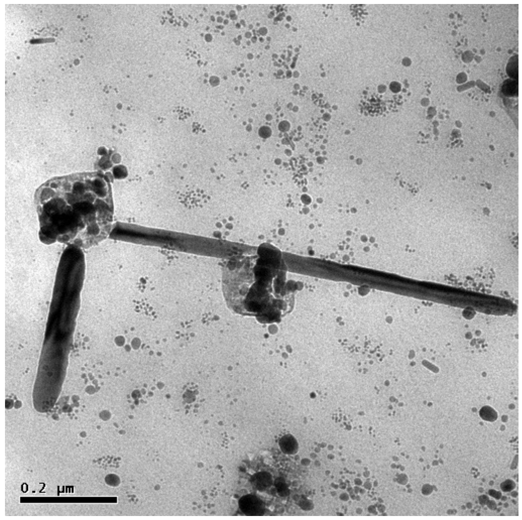

You can't measure it, if you can't detect it

7

Small Particles: Catalysts, Nanomaterials , Quantum Structures

Nanomaterials and processes challenge our ability to understand them:

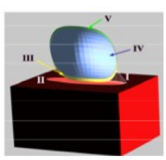

Catalytic Nanoparticles

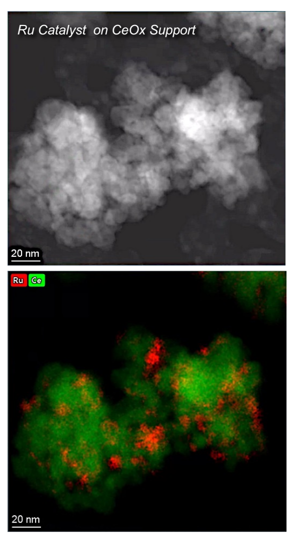

Key Challenges:

- Quantification - nanocrystallography at atomic resolution (automated w/ real time modeling and simulation)
- Atomic scale 3D imaging and diffraction
- In situ: controlled environments for simultaneous imaging and spectroscopy during reactions
- Dynamics: real-time observation

8

Spectroscopic Detectability Limits

Signal in the Presence of Background

Detectability is related our ability to measure the change in signal that is statistically significant above random flucutations

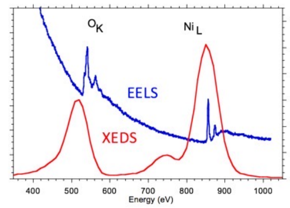

Student T-test Criterion

$$\Delta I > 2.33 * \sigma = 2.33 * \sqrt{I + B}$$

$$\frac{\Delta I}{I} > \frac{2.33}{\sqrt{\frac{I^2}{I + B}}}$$

if B <<I or I << B or we can define the minimum detectable mass & mass fractional as:

$$MDM \sim \frac{2.33}{\sqrt{I}}$$

$$\boxed{MMF \sim \frac{2.33}{\sqrt{I * \left[\frac{I}{B}\right]}}}$$

Notice the functional dependance on both I and I/B
This is not the traditional definition that has been used

In the past only the I/B has been used as a measure to identify conditions for highest "sensitivity" today that is no longer appropriate because of the changes in our detector technologies.

Both cases you want to maximize I and minimize I/B

9

Detectability is Based on a Signal Measurement

$$I_x = f(Z, E_o, t, \eta_o, \tau, \varepsilon, \Omega, \theta \ldots)$$

Minimum Detectable Mass

$$MDM \sim \frac{k}{I_x \cdot \eta_o \cdot \tau}$$

Minimum Mass Fraction

$$MMF \sim \frac{k}{\sqrt{I_x \cdot \left[\frac{I_x}{B_x}\right] \cdot \eta_o \cdot \tau}} =$$

k = Constant … 2.33 (Student T-test)
I_x = Characteristic (Peak) Signal from X
(I_x/B_x) = Peak to Background ratio for X
η_o = Incident electron flux
J_o = Incident electron current density
d = Probe diameter
τ = Analysis time

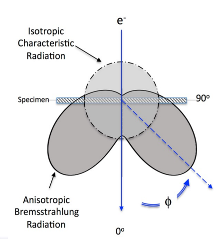

10

Bremsstrahlung Emission due to electron excitation

$$I_{Bgnd}\left(\phi, E_o, E_{Bgnd}, Z, \ldots\right) = I_\phi \bullet \left\{ \frac{C_z \bullet N_o \bullet \rho}{W_Z} \right\} \bullet \xi_o \bullet t \bullet \varepsilon_{Bgnd} \bullet \left\{ \frac{dE_{Bgnd} \bullet d\phi}{E_{Bgnd}} \right\}$$

$$I_\phi = I_i \bullet \left\{ \frac{\sin^2(\phi)}{[1-\beta \bullet \cos(\phi)^4]} \right\} + I_j \bullet \left\{ 1 + \frac{\cos^2(\phi)}{[1-\beta \bullet \cos(\phi)]^4} \right\}$$

$$I_i, I_j \Rightarrow f(Z, E_o, E_{Bgnd}, \ldots.), \qquad \beta = \frac{v}{c}$$

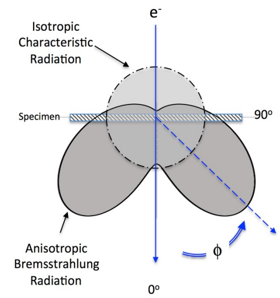

I_{Bgnd} =Bremsstrahlung intensity
E_o = incident electron energy (),
ϕ = observation angle
E_{Bgnd}, dE_{Bgnd} the continuum x-ray energy being measured and its window
I_i, I_j = continuum radiation components

Note: Traditional Detector Elevation Angle $\theta_E = \phi - 90$

Sommerfeld, 1931; Scherzer, 1932, Motz and Placious, 1958

11

Bremsstrahlung at fixed Background Energy window (7.48 keV) vs E_o

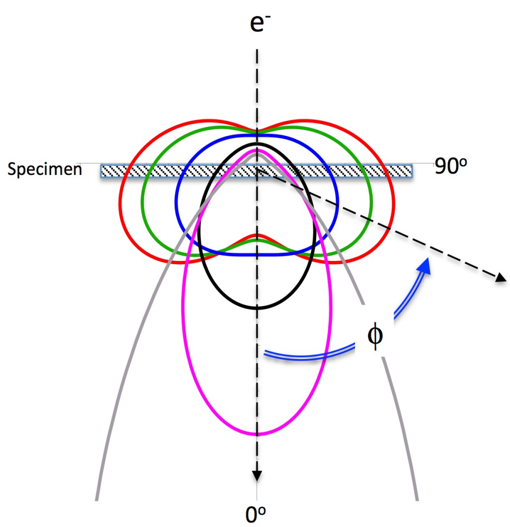

Eo (keV)	Vo (kV)
9.71	10
11.59	12
18.88	20
43.51	50
76.78	100
123.52	200
E_{Bgnd} = 7.48 keV	

Calculations for Ni

12

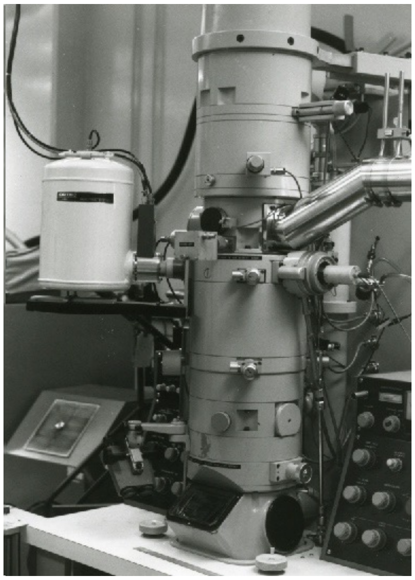

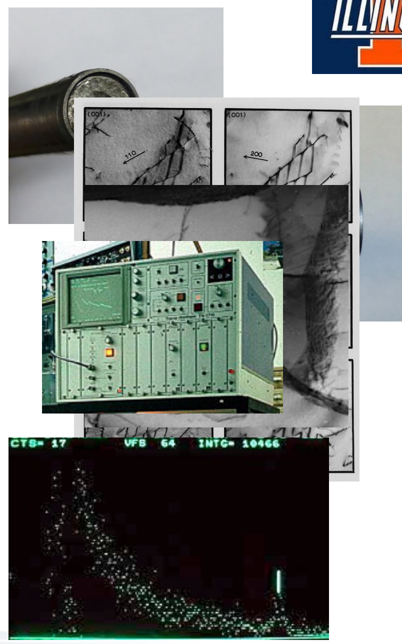

Hamish Fraser, John Woodhouse,...

13

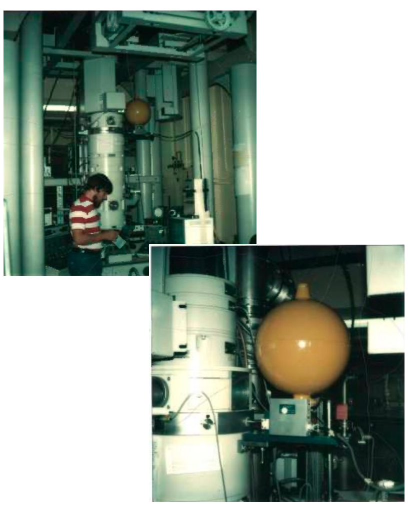

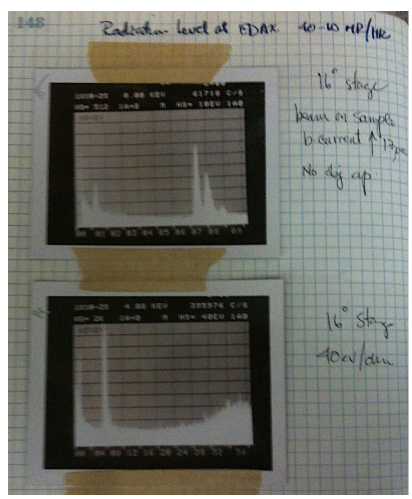

Ray Carpenter, Jim Bentley, Ed Kenik ...

14

Geometries Vary

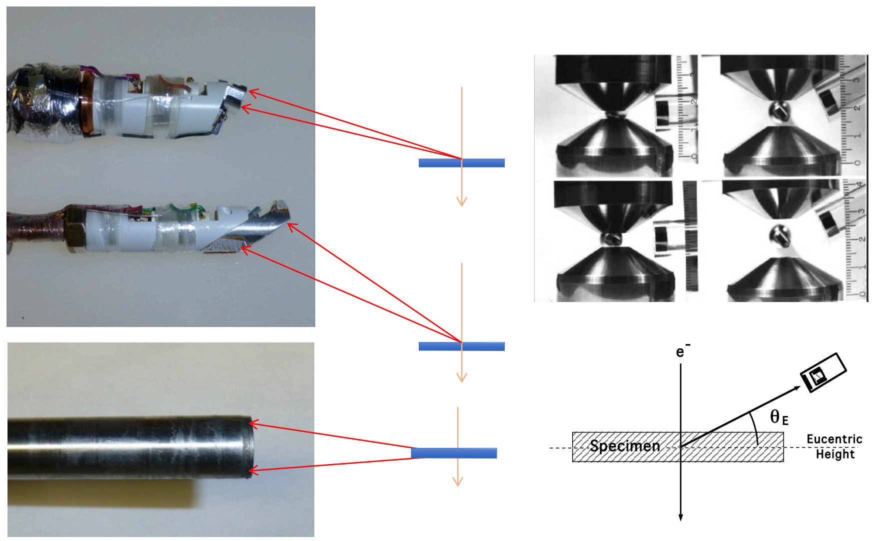

Hartmut Wiedersich, Charlie Allen, Mark Kirk, Dean Miller, Russ Cook, JG Wen……

15

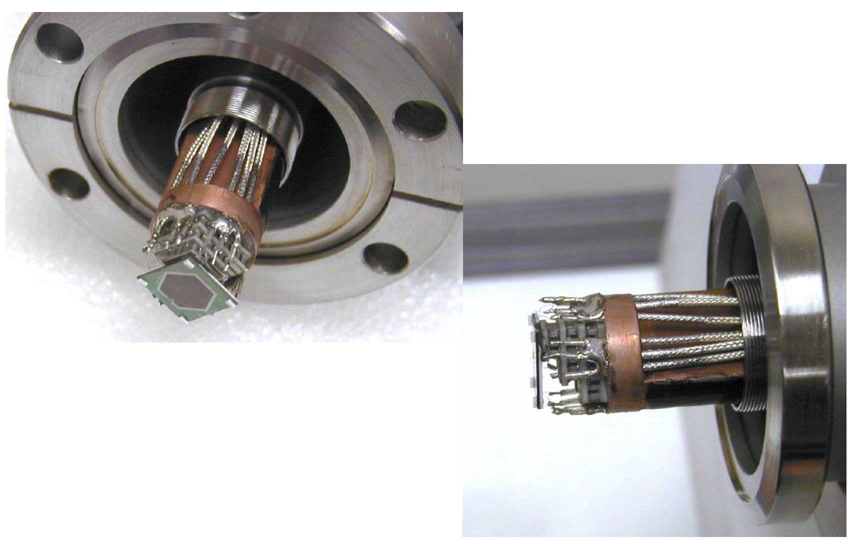

16

Detectors come in various sizes and shapes

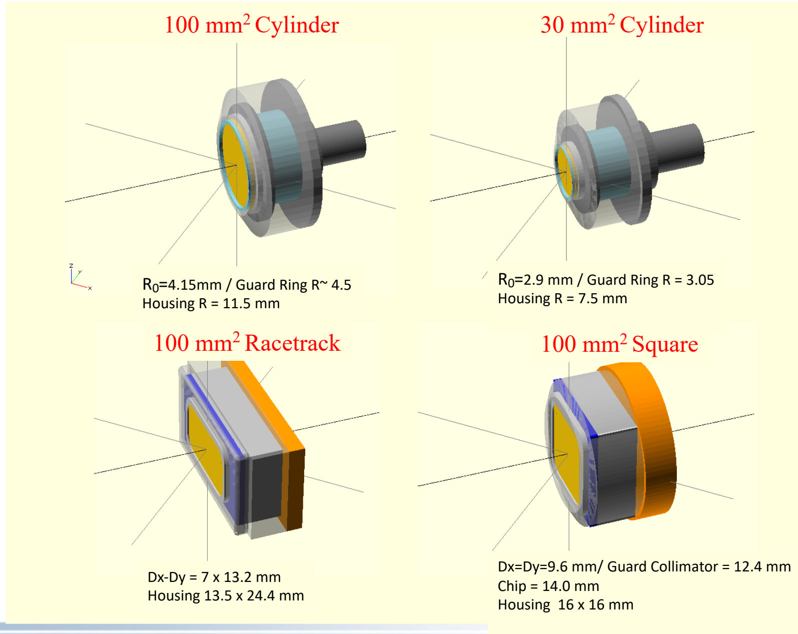

17

$$Intensity = \Gamma_{scatteringprobability} \bullet N_{atoms} \bullet \eta_{electrons} \bullet \tau_{time} \bullet \Omega_{efficiency}$$

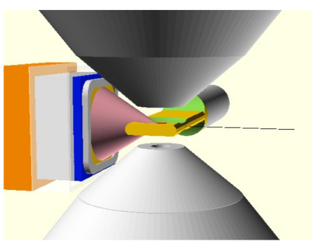

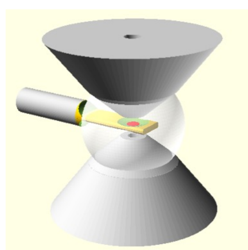

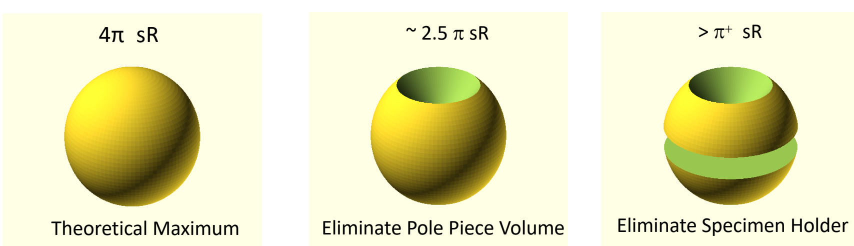

18

Non Traditional Geometries

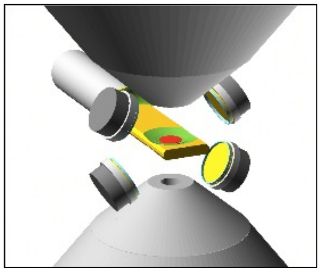

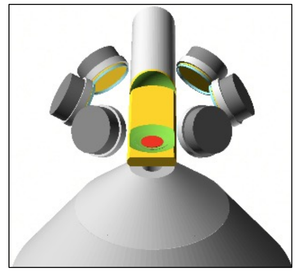

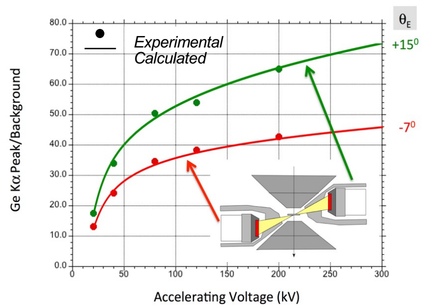

19

Traditional XEDS/AEM Geometry
Additional Limitations?

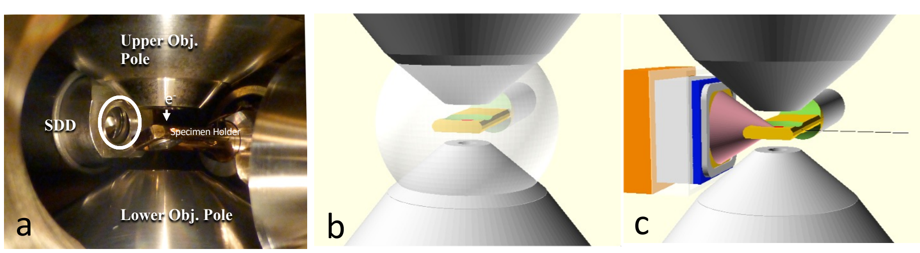

$$MDM \sim \frac{2.33}{\sqrt{T}}$$

20

SDD Geometries are extremely varied today

Using the simple tilt series protocol, individual configurations can now be directly characterized and compared on equal and unbiased basis.

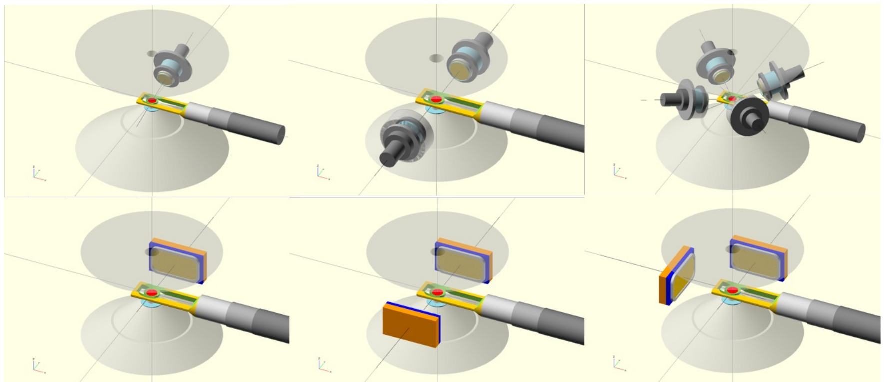

21

Penumbra of the specimen holder
is a limiting factor for XEDS in virtually all experiments
How do you determine it’s real extent and minimize it or correct for it?

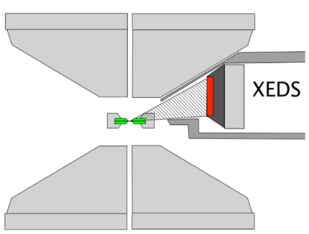

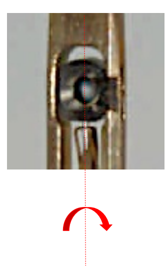

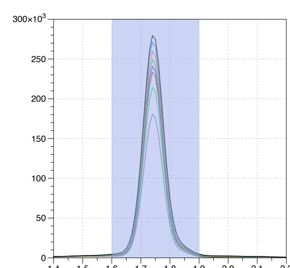

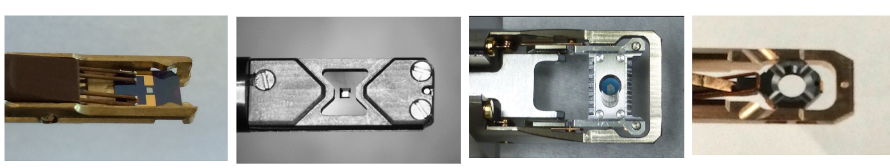

22

Germanium on SiN_x

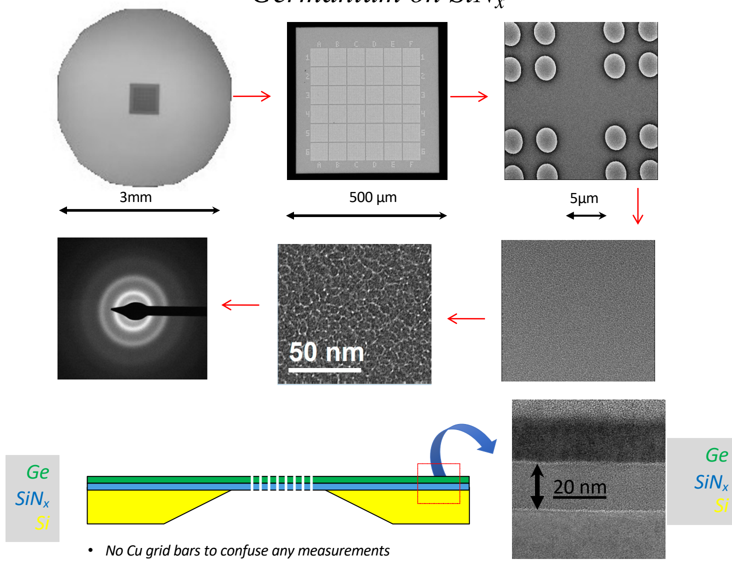

- *No Cu grid bars to confuse any measurements*
- *Holes allow beam current without removing the holder*
- *No crystalline channelling effects to complicate interpretation*

FIB Cross-section

Ref: Zaluzec, N. (2022). Quantitative Assessment and Measurement of X-ray Detector Performance ...... Microscopy and Microanalysis, 28(1), 83-95. doi:10.1017/S143192762101360X,

23

Penumbra/Geometry of the Specimen Holder is also Critical

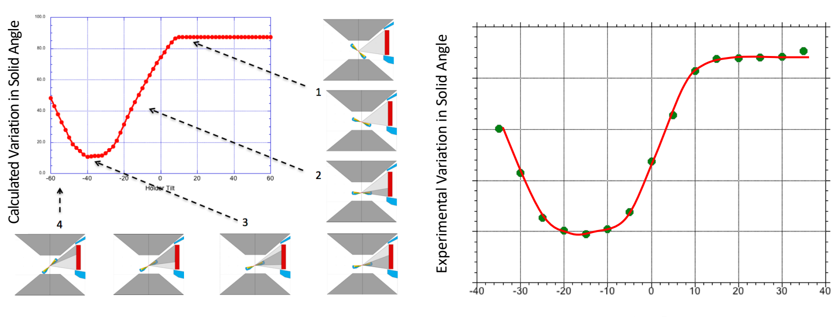

Calculation of Holder Tilt to Minimize Holder and Detector Penumbra

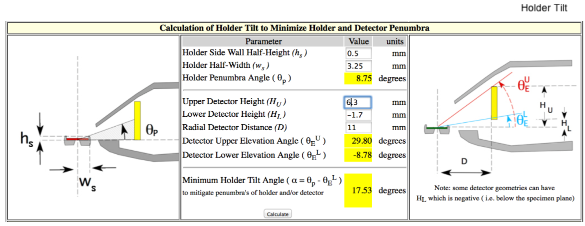

Parameter	Value	units
Holder Side Wall Half-Height (h_s)	0.5	mm
Holder Half-Width (w_s)	3.25	mm
Holder Penumbra Angle (θ_p)	8.75	degrees
Upper Detector Height (H_U)	6 3	mm
Lower Detector Height (H_L)	-1.7	mm
Radial Detector Distance (D)	11	mm
Detector Upper Elevation Angle ($\theta_E{}^U$)	29.80	degrees
Detector Lower Elevation Angle ($\theta_E{}^L$)	-8.78	degrees
Minimum Holder Tilt Angle ($\alpha = \theta_p - \theta_E{}^L$) to mitigate penumbra's of holder and/or detector	17.53	degrees

Calculate

http://zaluzec.com/NJZTools/

24

Absolute Comparisons are now possible
As long as you also measure Beam Current
& Live times

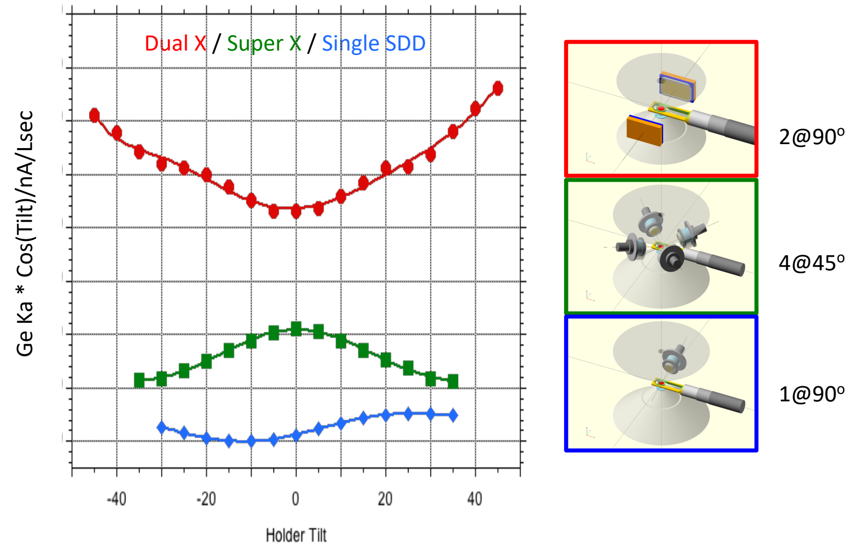

25

XPAD - X-ray Perimeter Array Detector

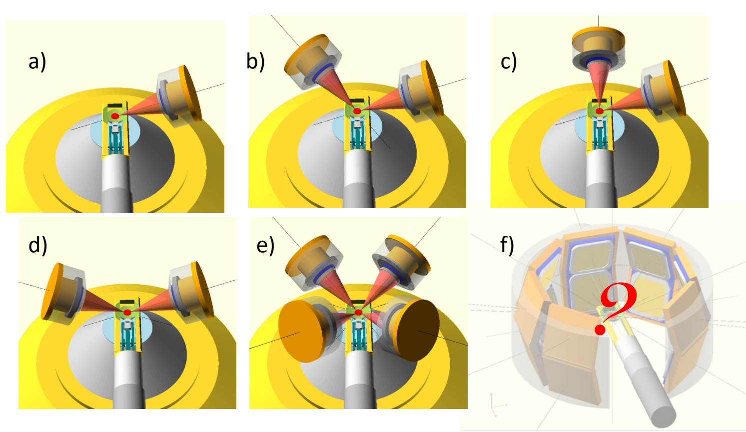

Microsc. Microanal. V 20, 1318–1326, 2014
Ultramicroscopy , V 151, 2015, Pages 240-249

26

ANL/UofC PicoProbe

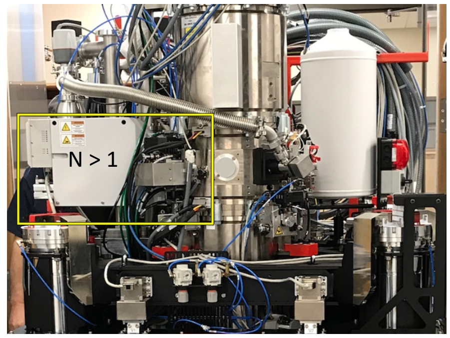

ANL LDRD Projects
ANL/ThermoFisher(FEI) CRADA #1300701

ThermoFisher SCIENTIFIC

27

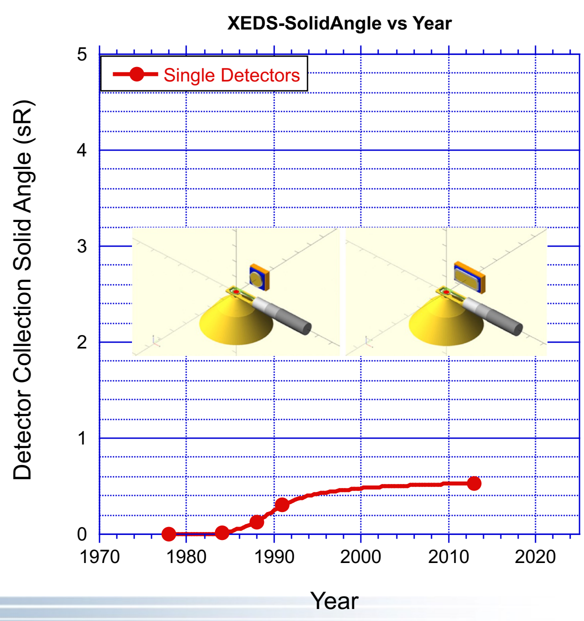

28

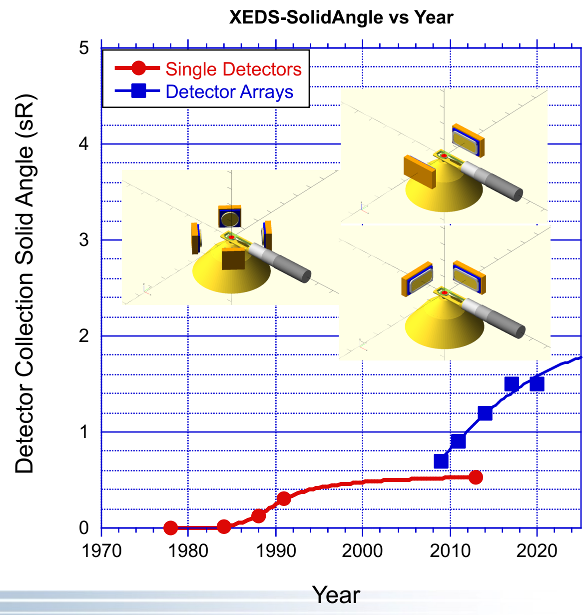
XEDS-SolidAngle vs Year
Single Detectors
Detector Arrays
Detector Collection Solid Angle (sR)
0
1
2
3
4
5
1970
1980
1990
2000
2010
2020
Year

29

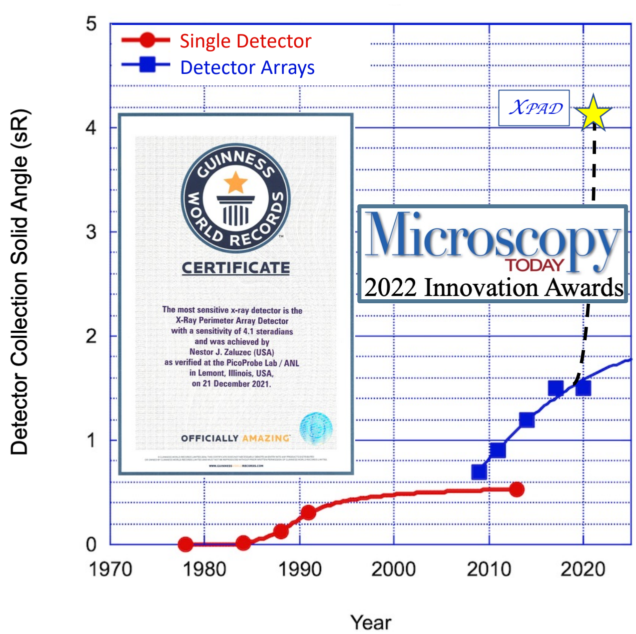
Single Detector
Detector Arrays
XPAD
GUINNESS WORLD RECORDS
CERTIFICATE
The most sensitive x-ray detector is the X-Ray Perimeter Array Detector with a sensitivity of 4.1 steradians and was achieved by Nestor J. Zaluzec (USA) as verified at the PicoProbe Lab / ANL in Lemont, Illinois, USA, on 21 December 2021.
OFFICIALLY AMAZING
Microscopy TODAY
2022 Innovation Awards
Detector Collection Solid Angle (sR)
0
1
2
3
4
5
1970
1980
1990
2000
2010
2020
Year

30

Analytical PicoProbe Arrival –> Assembly –> First Light

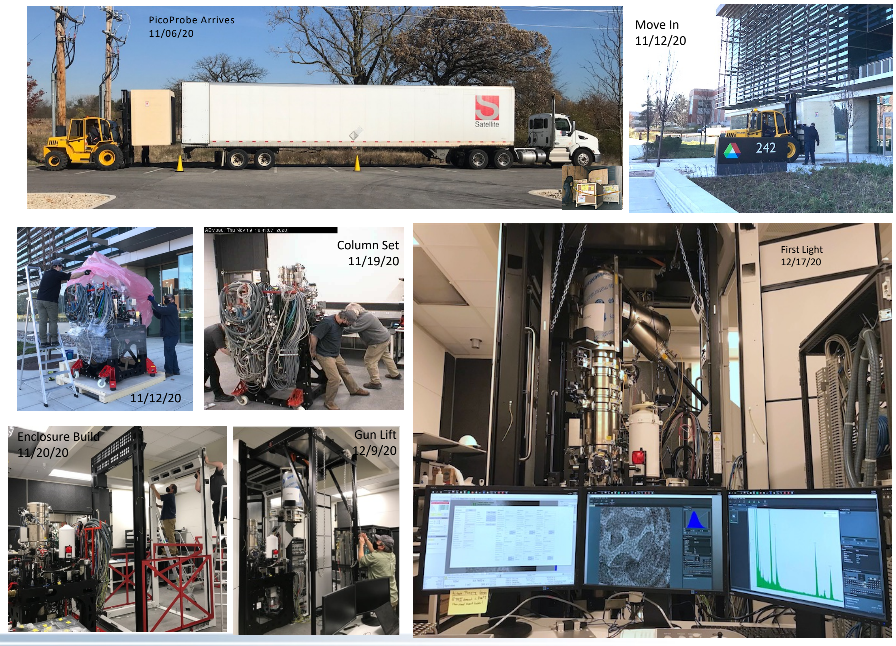

31

Comparisons of Performance
Test Specimen: Ge on SiNx

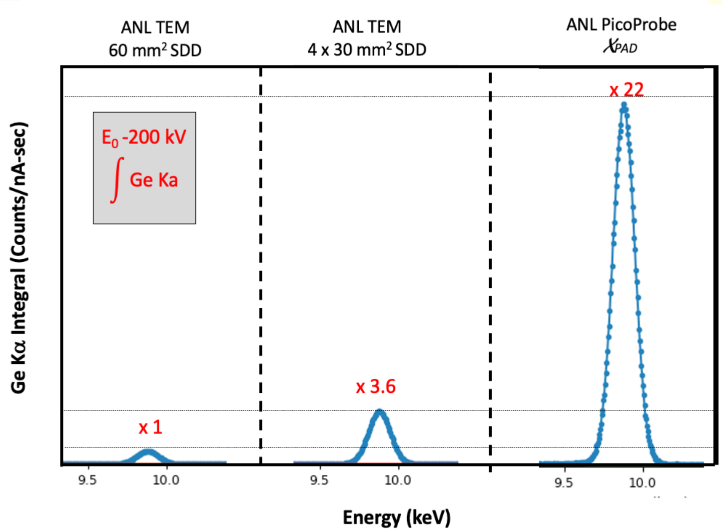

Ge/SiNx Specimen : http://www.temwindows.com/category_s/55.htm

Protocol for XEDS System Penumbra Measurements:
Zaluzec etal Microsc. Microanal. 22 (Suppl 3), 2016, 278-279

32

Quantitative Detector Configuration Comparisons

$$\Omega = 4\pi \cdot \frac{I_{K\alpha}}{\{\sigma_K \cdot \omega_K \cdot \Gamma_{K\alpha}\} \cdot \left\{\frac{C_Z \cdot N_O \cdot \rho_Z}{W_Z}\right\} \cdot t_Z \cdot \eta_o \cdot \tau \cdot \varepsilon_{K\alpha}}$$

Detector Configuration	Experimental Ge Ka Intensity (Integrated counts/nA-sec)	Theoretical Cross-section (Barns)	Experimental Ω (sR)
Single 60 mm² SDD	610	157.8-182.7	0.18-0.16

$I_{K\alpha}$ = Net integrated full Kα peak intensity
σ_K = Kth shell x-ray ionization cross-section
ω_K = Kth shell x-ray fluorescence yield
$\Gamma_{K\alpha}$ = Radiative partition function for the Kα signal
C_Z = Composition of the volume producing the signal
N_o = Avagodro's Number
ρ_Z = Density of the volume producing the signal
W_Z = Atomic weight of the species producing the signal
t_Z = Thickness the volume producing the signal
η_o = Incident electron beam current
τ = Acquisition live time
$\varepsilon_{K\alpha}$ = X-ray detector efficiency for $I_{K\alpha}$.

33

$$I_\alpha = \{\sigma_\alpha(E_o, Z) \bullet \Gamma_\alpha \bullet \omega_\alpha\} \bullet \left\{\frac{C_Z \bullet N_o \bullet \rho}{W_Z}\right\} \bullet \xi_o \bullet t \bullet \left\{\varepsilon_\alpha \bullet \frac{\Omega}{4\pi}\right\}$$

Accelerating Voltage (kV)	Average Ge Ka Intensity (Integrated counts/nA-sec)	Theoretical Cross-section (Barns)	Experimental Ω (sR)
200	15570	157.8-182.7	4.28 ± 0.3
300	15160	144.0-167.5	~ 4.55 ± 0.3

Experimentally determined solid angle for XPAD on the ANL PicoProbe. The designed solid angle was 4.47 sR and is within the errors of the cross-section models] used.

Zaluzec N.J. , (1984) "K and L Shell Cross Sections for X-ray Microanalysis in an AEM" Analytical Electron Microscopy, ed. D. Williams, San Francisco Press, 279-284,

Llovet, X, Powell, C.J., Salvat, F. and Joblonski A, (2014) "Cross Sections for Inner-Shell Ionization by Electron Impact, Journal of Physical and Chemical Reference Data 43, 13102

34

HyperSpectral Image Carbide Precipitates in Type 709 Steel

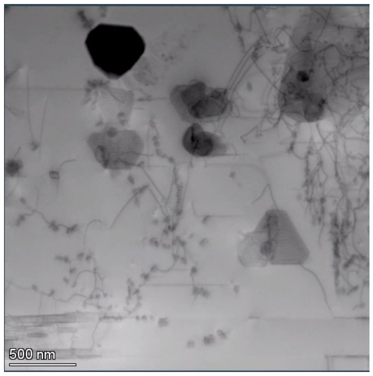

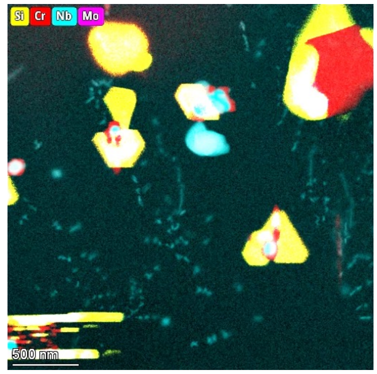

ElectroPolished Type 709 Steel
ANL PicoProbe/XPAD
300 kV, 400 pA @ 40 kX
2K x 2K @ 13.7 ms/pixel
Conventional background subtracted
0.7 pixel Gaussian Blur to minimize noise

35

Atomic Channeling and HyperSpectral Imaging

β – NiAl [001]   *HAADF*

288 pm

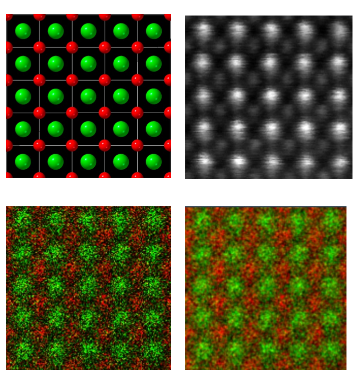

400usec/pixel single frame   2.4msec/pixel 6 frames

Structure Type:	Crystal
Chemical Formula:	β – NiAl
Z:	1
Space Group:	$P\,m\,\bar{3}\,m$
Crystal System:	Cubic
a:	2.8810 Å
Cell Volume:	23.913 Å³
Asymmetric Unit:	2 sites
Unit Cell:	2 sites/unit cell
Density:	5.9505 g/cm³
Visible Sites:	97

1pA-usec ~ 6.24 electrons => 50 pA @ 400 usec ~ $1.2\text{x}10^5$ electrons
Note: this measurement was grossly oversampled @ 26pm/pixel

20210930

36

GaAs {110}

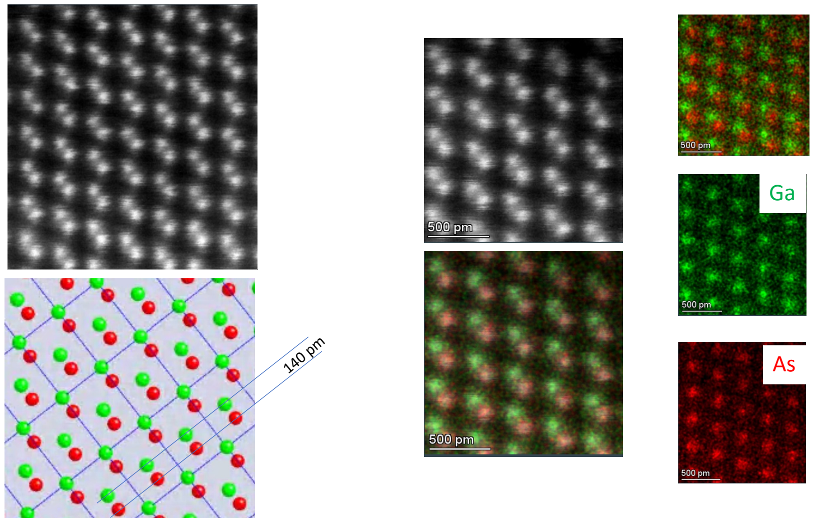

200kV / 40 pA ~ 180 x 180 pixels
330usec/pixel @ 10 frames => ~ 300msec/frame

37

Evolving Detectors & Geometries for XEDS
Collection Efficiencies have Significantly Increased this year

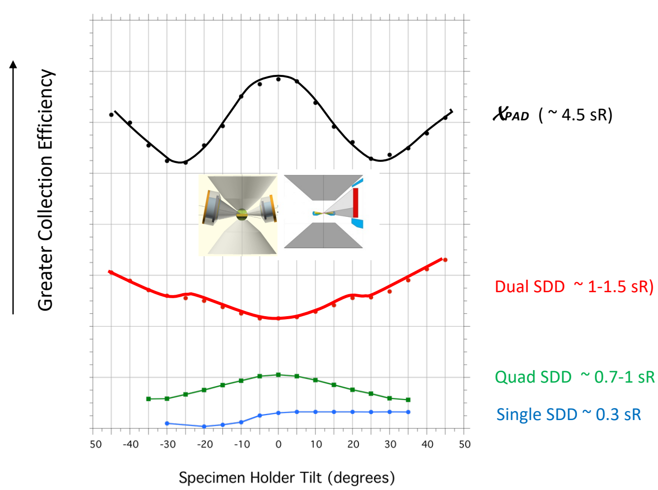

Protocol for XEDS System Penumbra Measurements:
Zaluzec etal Microsc. Microanal. 22 (Suppl 3), 2016, 278-279

38

Detectability is Based on a Signal Measurement

$$I_x = f(Z,\ E_o,\ t,\ \eta_o,\ \tau,\ \varepsilon,\ \Omega,\ \theta \ldots)$$

Minimum Detectable Mass

$$MDM \sim \frac{k}{I_x \cdot \eta_o \cdot \tau}$$

Minimum Mass Fraction

$$MMF \sim \frac{k}{\sqrt{I_x \cdot \left[\frac{I_x}{B_x}\right] \cdot \eta_o \cdot \tau}} =$$

k = Constant … 2.33 (Student T-test)

I_x = Characteristic (Peak) Signal from X

(I_x/B_x) = Peak to Background ratio for X

η_o = Incident electron flux

J_o = Incident electron current density

d = Probe diameter

τ = Analysis time

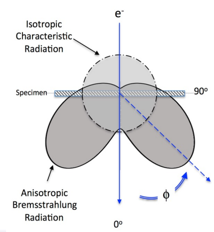

39

Spectroscopic Detectability Limits

Signal in the Presence of Background

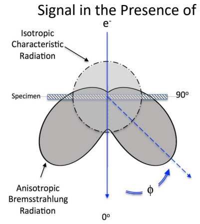

$$I_\alpha = \{\sigma_\alpha(E_o, Z) \bullet \Gamma_\alpha \bullet \omega_\alpha\} \bullet \left\{\frac{C_Z \bullet N_o \bullet \rho}{W_Z}\right\} \bullet \xi_o \bullet t \bullet \left\{\varepsilon_\alpha \bullet \frac{\Omega}{4\pi}\right\}$$

$$I_{Bg} = I_i \bullet \left\{\frac{\sin^2(\phi)}{[1-\beta \bullet \cos(\phi)^4]}\right\} + I_j \bullet \left\{1 + \frac{\cos^2(\phi)}{[1-\beta \bullet \cos(\phi)]^4}\right\}$$

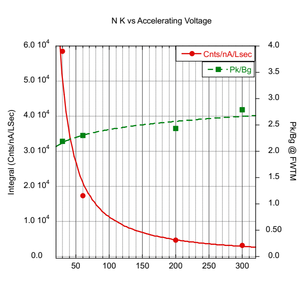

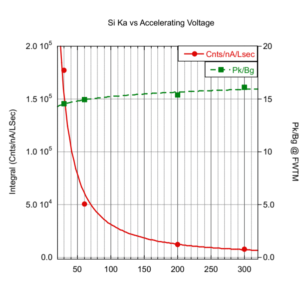

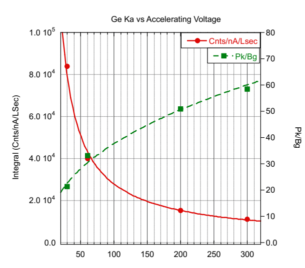

$I_K \uparrow$ as $E_o \downarrow$ $\quad MDM \sim \frac{2.33}{\sqrt{T}}$ $\quad \frac{I_K}{I_{Bg}} \downarrow$ as $E_o \downarrow$ $\quad MMF \sim \frac{2.33}{\sqrt{I * \left[\frac{I}{B}\right]}}$

40

Analytical Sensitivity $\neq \frac{I_K}{I_{Bg}}$

$$\frac{\Delta I_K}{I_K} = \frac{2.33}{\sqrt{\frac{I_K{}^2}{I_K + Bgnd}}}$$

$\frac{\Delta I_K}{I_K}$ (MMF) ⬇ as E_o ⬇ (i.e. sensitivity gets better)

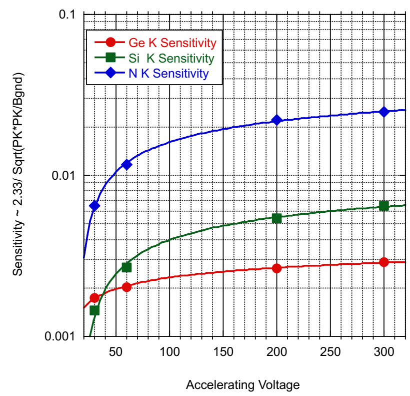

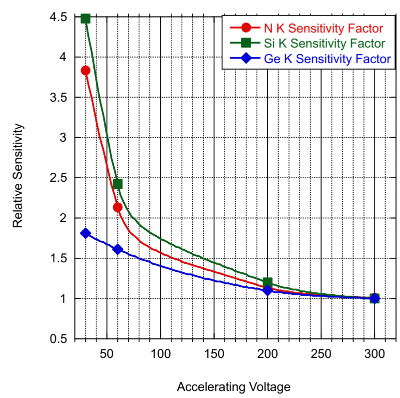

41

MMF Improvements Improves ~ x10

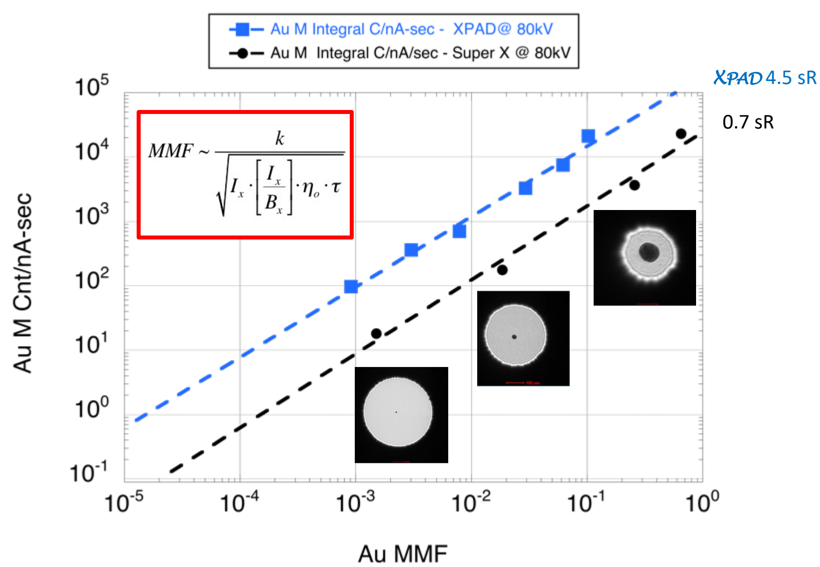

42

20211106xx-07xx -HEA - CrMnFeCoNi
Irradiated 1MeV Kr -@ 500ºC @ 1dpa Near {110} Zone

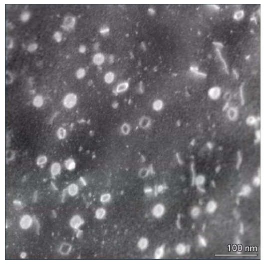

DF STEM

BF STEM

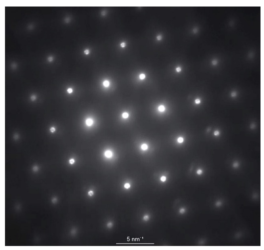

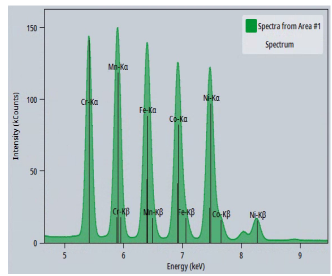

43

2021110611 -HEA - CrMnFeCoNi
{110} Zone
Edge on 1/3 <111> Loop

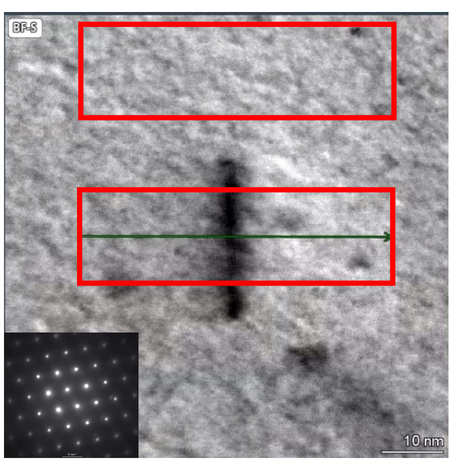

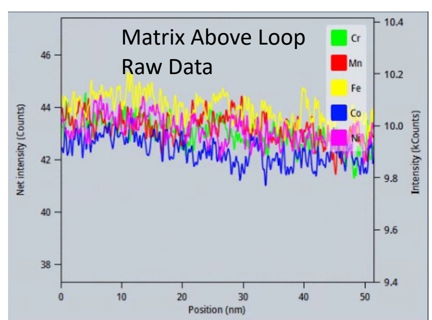

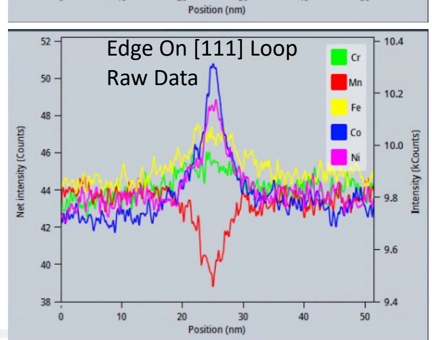

Co Ni enriched - Mn Depleted,

44

2022054 –Ordered HEA – $Al_{0.3}CrFeCoNi$
{001} Zone
1/3 <111> Loops

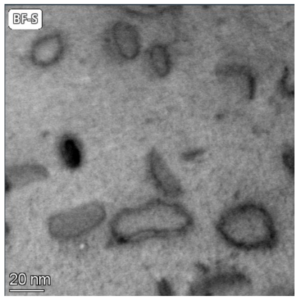

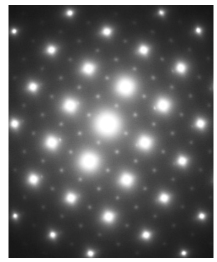

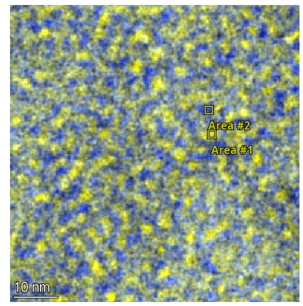

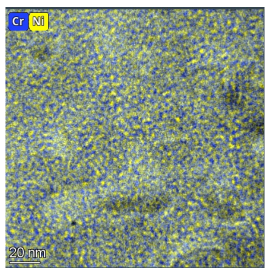

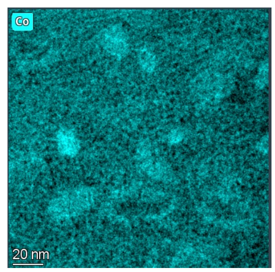

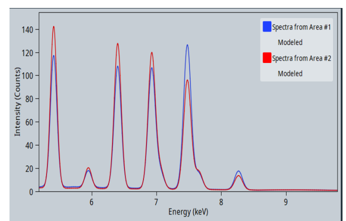

45

2022050508 –Ordered HEA – $Al_{0.3}CrFeCoNi$
{110} Zone
Edge on 1/3 <111> Loop

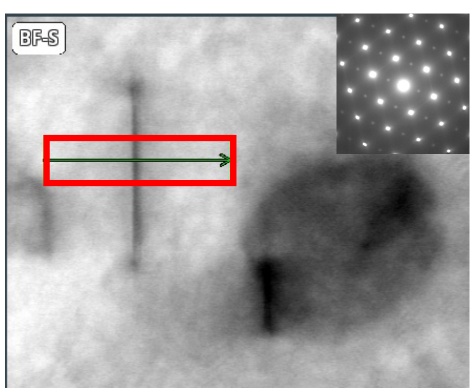

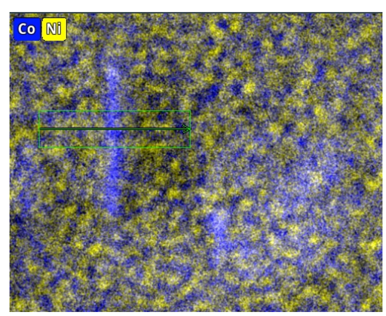

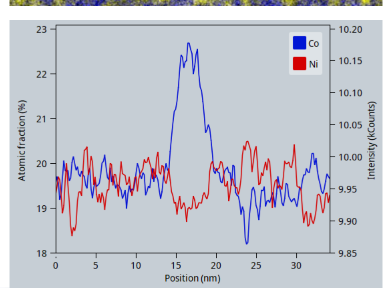

46

2022050508 –Ordered HEA – $Al_{0.3}CrFeCoNi$
{110} Zone
Edge on 1/3 <111> Loop

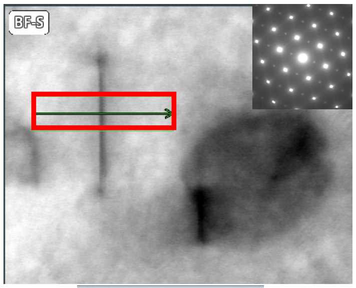

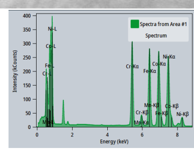

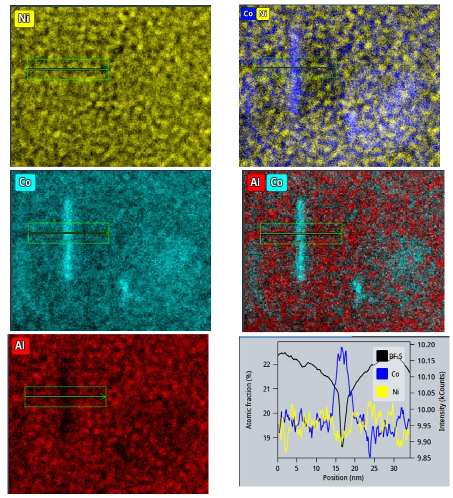

47

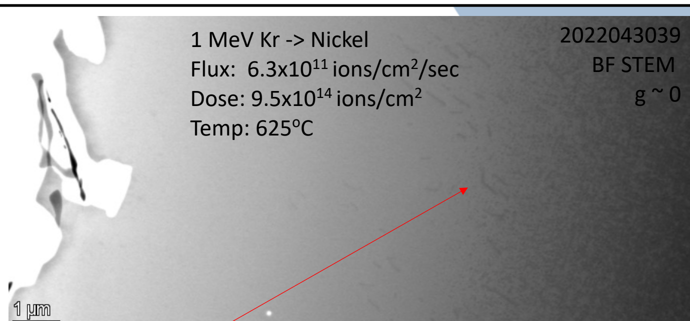

1 MeV Kr -> Nickel
Flux: $6.3x10^{11}$ ions/cm^2/sec
Dose: $9.5x10^{14}$ ions/cm^2
Temp: 625°C

2022043039
BF STEM
g ~ 0

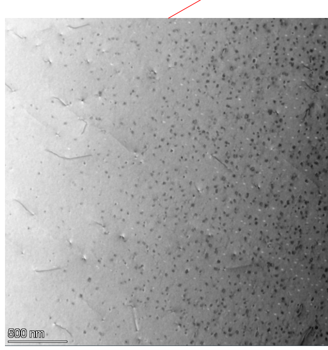

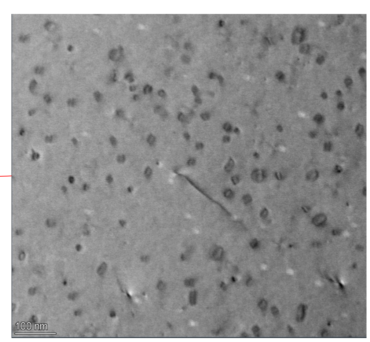

Edge of Damage Zone

g ~ 0 loops in contrast, bubbles present

48

XEDS Spectra from Bubbles

20220430-Ni/Zr

PicoProbe
300kV
200pA
100Lsec
~ 2 nm probe

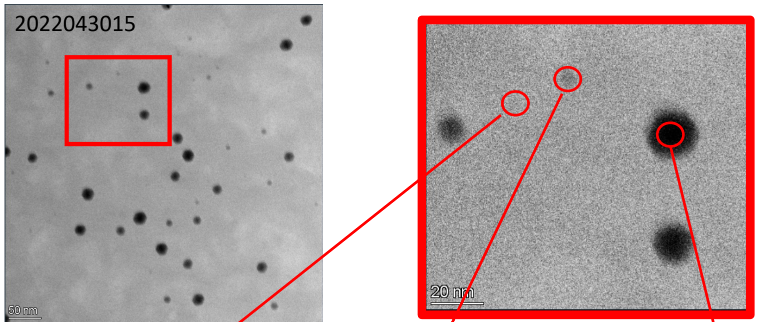

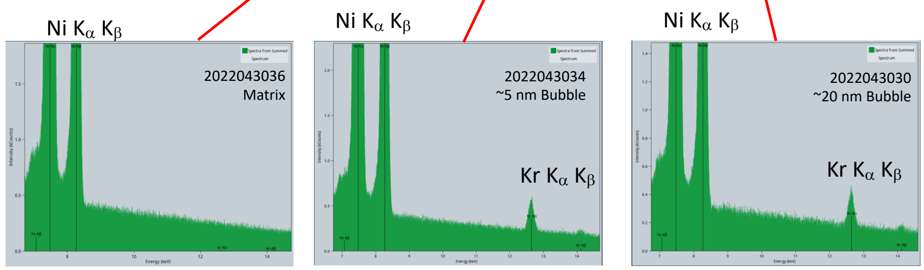

Kr/Ni = 0.003

49

If you can't detect it, then you can't measure it.

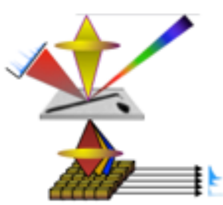

Thanks !

Questions ?

Zaluzec @aaem.amc.anl.gov
Zaluzec@Microscopy.com

50

51

The PSC Analytical PicoProbe Electron Optical Beam Line

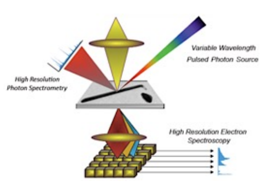

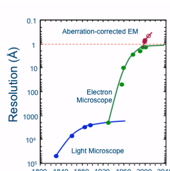

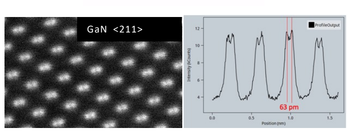

<211> GaN sub-atomic image
Ga-Ga = 63 pm

Key Features/Attributes at Commissioning

- E_0: 30-300 kV Electron Source
- High Brightness Coherent Field Emission Gun
- Probe Corrector ($\delta x < 55$ pm)
- Monochromator ($\delta E \lesssim 30$ meV)
- XPAD 4.5 sR X-ray Spectrometer
- ZTwin Lens
- Next Generation Multi-Port Octagon
- HR/LowDrift Piezo Goniometer
- 4Kx4Kx16 bit CMOS Imaging Detector
- 128x128x30bit Diffraction Camera
- CTEM/STEM/iDPC /4DSTEM Modes
- Analytical LBHV DTilt Holder
- Ambient Tomography Holder
- Pytchography/Tomography Holder
- Ambient Liquid Cell Holder
- Cryo Tomography/Spectroscopy Holder
- Dynamic Imaging ~ 0-300 fps
- Multi-Modal Enabled
- Telepresence Enabled
- Electron Energy Filter / UltraMono - Spring 2023

Image Resolution
CTEM < 100 pm / STEM ~ 55 pm
Temporal Resolution
0- 300+ fps (CTEM) $\lesssim$ 1 usec/pixel (STEM)
Spectroscopy
- Worlds most sensitive AEM XEDS detector (>4sR)
- HR Energy Filter-Spectrometer - (< 30 meV)
Environmental
Commercial and Custom (Ambient) in-Situ Holders
Direct Electron Detectors
Cryo EM Imaging for Soft/Hard, Energy & Quantum Materials
Cryo EM Prep / Inert transfer
Future
In-situ Gaseous Media @ Temperature
In-situ Photonics/UV/IR/NIR
Adative Holographic Optics

ANL/ThermoFisher
CRADA #1300701
ANL LDRD #2017-153
ANL PRJ# 1006014
NSF MRI #2117896

52

Today's XEDS Geometries

0.1-0.5 sR

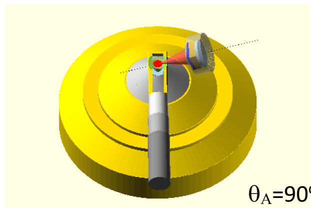

$\theta_A = 90^o$

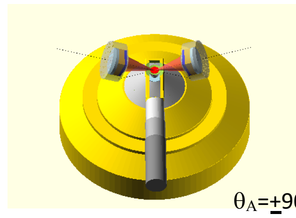

$\theta_A = \pm 90^o$

0.5-1.5 sR

0.5-1 sR

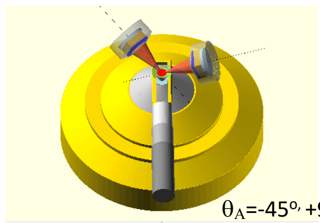

$\theta_A = -45^o, +90^o$

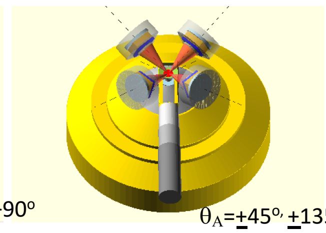

$\theta_A = \pm 45^o, \pm 135^o$

0.7-0.9 sR

53